A model experiment to assess the effects of inclusions on wave propagation in soil media

Une expérience modèle pour évaluer les effets d'inclusions sur le signe propagation dans les mass-média de sol

T. W. Houston & R. P. Ray

Department of Civil & Environmental Engineering, University of South Carolina

ABSTRACT

A data acquisition system has been assembled using Micro-Electro-Mechanical Systems (MEMS) technology which provides a flexible data gathering capability to support recording accelerations at various locations within a sand filled 5 meter square test pit that has a depth extending into underlying gravelly soils. Dual-axis accelerometers weighing less than 1 gram each, made possible by advances in MEMS technology, are connected to up to 5 data acquisition (PXI modules) boards, each capable of controlling and recording data from 16 separate dual axis accelerometers. This data acquisition system is used to measure and record acceleration data from wave propagations that are generated by the impact of a hammer on a striker plate and are modified by an inclusion or occlusion buried in the soil media. Thirty-four two-axis accelerometers were placed at surface and embedded locations on either side of various inclusions buried in the test pit. This large number of accelerometers permits experimentally obtaining high quality spatial and temporal data that can describe the character of the generated wave-forms and the modification of those wave-forms caused by the inclusion. A number of differing materials and geometric forms are used to create inclusions in order to provide sufficient data to permit ascertaining the ability of the measurements to describe the character of the inclusion. Continuous Wavelet Transforms are used to remove background noise and to aid interpretation of the character of the generated wave-form.

RÉSUMÉ

Un système d'acquisition de données a été monté en utilisant la technologie des systèmes micro-électromécaniques (SMEM) qui fournit une capacité de cueillette de données flexible pour supporter l'enregistrement d'accélérations en divers endroits dans un puits d'essai de 5 mètres carrés emplis de sable et ayant une profondeur atteignant les sous-couches de sols graveleux. Des accéléromètres à deux axes pesant moins de 1 gramme chacun, construits grâce à la progression de la technologie SMEM, sont raccordés à jusqu'à 5 plaquettes (modules PXI) d'acquisition de données chacune étant capable de contrôler et d'enregistrer les données de 16 accéléromètres à deux axes indépendants. Ce système d'acquisition de données est utilisé pour mesurer et enregistrer les données d'accélération des ondes de propagation qui sont générées par l'impact d'un marteau sur une plaque de percussion et qui sont modifiées par une inclusion ou une occlusion enfouie dans les substances du sol. Trente-quatre accéléromètres à deux axes ont été placés à la surface et dans des endroits incrustés de chaque côté de diverses inclusions enfouies dans le puits d'essai. Ce grand nombre d'accéléromètres permet d'obtenir par expérience des données spatiales et temporelles de haute qualité qui peuvent décrire le caractère des formes d'onde générées ainsi que leurs modifications causées par l'inclusion. Un nombre de différents matériaux et formes géométriques est utilisé pour créer des inclusions afin de fournir suffisamment de données pour permettre l'évaluation de la capacité des mesures à décrire le caractère de l'inclusion. Des transformées en ondelettes continues sont utilisées pour éliminer le bruit de fond et pour aider à l'interprétation du caractère de la forme d'onde générée.

Keywords : wave propagation, wavelets, soil, inclusions

1 INTRODUCTION

Shokouhi, et. al. (2005) studied the use of wavelets to describe the response of media containing softer and stiffer material as well as various shaped voids. The studies used computed surface motions based on the results of axi-symmetric finite element analyses that modeled the response of a homogeneous, elastic media. They used wavelets to study surface response at selected locations (simulating transducer recordings) preceding, directly above, and following inclusions or void space. The purpose of our work is to extend the use of wavelets from their analysis to results obtained from measurements in soil. A 5m x 5m x 3m deep sand pit at the Geotechnical Engineering laboratory at the University of South Carolina is used to perform the experiments.

In general, a limitation on the use of wavelets for data interpretation has been the lack of quantitative methods to evaluate the time series data. However, recent developments by Torrence and Campo (1998) provide a methodology that can be used to assess the results (coefficients) of the wavelet transform by comparing the power in a measured time history signal to the expected value of power from a white noise process. This method is easily extended to extract measured signals from any form of background noise. Thus the use of wavelets coupled with statistical significance testing has been utilized in this study to interpret and filter measured acceleration time histories.

The testing program consisted of placing accelerometers in the soil to measure wave travel at the surface and at depth. Due to the small scale of the experiment and required precision of measurement, high frequency signals (for geotechnical engineering) were necessary. A high performance data

Proceedings of the 17th International Conference on Soil Mechanics and Geotechnical Engineering
M. Hamza et al. (Eds.)

doi:10.3233/978-1-60750-031-5-668

acquisition system and careful experimental design was necessary. Measured accelerations were obtained by applying a pulse loading to a circular plate located at the center of the test pit and recording the wave as it propagated outward. Time histories were necessarily short to avoid reflections from the test pit's outer walls. Since the base of the pit is resting on natural soil, reflections from there were much less. Additionally the wave velocities of the underlying soil were much lower than in the pit itself so there was little chance for refractions to interfere with measurements. Wave forms measured for experimental cases having no inclusions were compared with wave forms measured for experimental cases having inclusions. For this paper, the inclusion discussed is a 15cm x 15cm x 76cm concrete beam buried 30cm into the soil.

2 DATA ACQUISITION SYSTEM

A data acquisition system (DAQ) has been assembled using Micro-Electro-Mechanical Systems (MEMS) technology. The MEMS technology are included in this system in the form of very compact (5mm x 5mm x 2mm), lightweight (less than 1gm) and low-cost (about $20 each) dual-axis accelerometers. They are wired to a modular electronic instrumentation platform (PXI) that provides a flexible data gathering capability for obtaining high quality measurements. The use of the PXI platform supports an easy integration of modules that are available from a large number of vendors. Control and management of the data acquisition for this experiment is accomplished by using an assembly of modular components provided by National Instruments (NI) combined with sensors obtained from other vendors (i.e. Analog Devices). The purpose of the data acquisition system described is to accommodate measurement of accelerations in the soil at a sufficient number of locations to accurately describe wave-forms as they propagate away from the source. When wave-forms are generated by a mechanical impact an electronic device marks the time of impact, simultaneously triggering the recording of data from all of the accelerometers, thus insuring that all measurements are base-lined to the same time datum.

The assemblage of components that comprise the DAQ system includes two-axis MEMS accelerometer (Analog Devices Model ADXL203) sensors, having a full-scale range of ± 1.7g, that are small and light enough to be embedded into the soil without creating significant interaction effects between the soil and the sensor. The trigger signal originates from a piezoelectric load cell. The load cell also senses the force-time history of the hammer blow. The steel striker plate, 1.27cm thick by 15.24cm diameter, rests at the center of the pit filled with sand. The accelerometers are connected to a shielded circuit board (NI Model SCB-68) using light gage shielded instrument wire, which is in turn connected to a multifunction data acquisition device (NI Model 6259M). This DAQ card is mounted in a 6-slot chassis (NI Model PXI-1036) that contains a controller (NI Model MXI-4) allowing a PC with appropriate software to control the data collection process; including setting trigger parameters, viewing signals as they are collected, and managing the data that is to be saved. This system is capable of obtaining one million samples per second (S/sec) from up to 80 dual-axis accelerometers, or from up to 160 sensors. This testing program recorded 1000 S/sec from each dual axis accelerometer permitting sampling of frequencies up to 500 Hz. The assembled system is shown schematically in Figure 1.

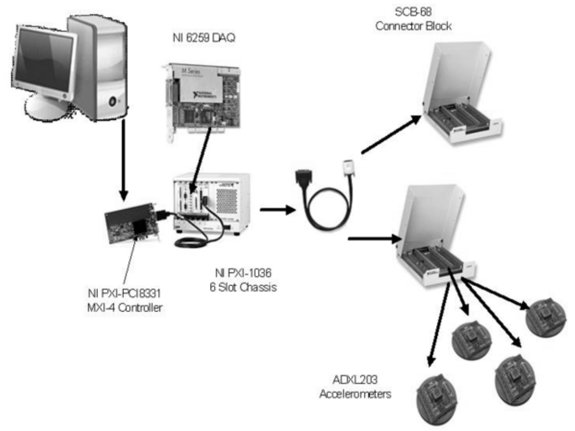

Figure 1: Schematic of Data Acquisition System

3 EXPERIMENTAL SETUP

The data acquisition system described is deployed in a sand pit 5m x 5m square that extends down to and gravel and filter fabric blank underlain by natural stream bank deposits of soft clay, silt and sand. The pit is filled with uniformly-graded sand having an approximate shear wave velocity of 180m/sec and compression wave velocity of 335m/sec. The objective of the data acquisition part of the experiment is to obtain acceleration wave-forms that contain high quality spatial and temporal data. Thus, a grid consisting of 34 accelerometers is deployed which includes surface sensors, and layers of sensors at 30cm and 60cm depths. Inclusions are placed in a "target zone" located between the sensors at 30cm and 91cm from the source. Inclusions consist of embedded bodies that have varying properties; size, material, and density. The input energy source is a slide hammer which strikes a load cell mounted on the steel plate resting on the sand surface. The test setup is shown in Figure 2.

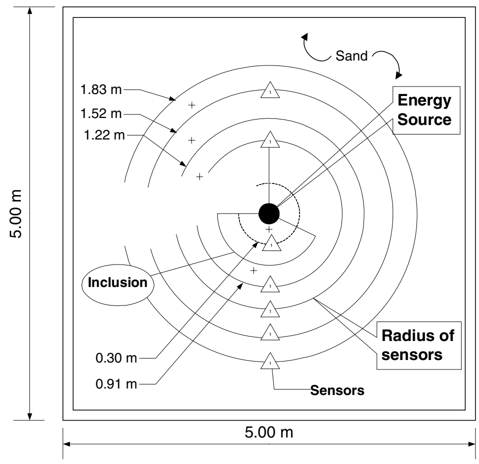

Figure 2: Test setup including sensor locations

4 EXPERIMENTAL RESULTS

Acceleration data is collected for vertical and horizontal (radial) directions at every sensor position in the grid described above. In addition, a force-time history measured at the load cell is recorded. The force-time history is shown in Figure 3.

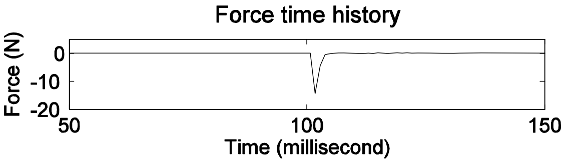

Figure 3: Force time history at source due to hammer strike

Measurements taken of the wave-form produced by the impulse load include the accelerations generated by the pulse as well as those generated from other sources including background (ambient) vibration, variation in the voltage measurements inherent to the measurement and recording instruments, and stray vibrations associated with the application of the pulse load. These variations in the measured accelerations not associated with the wave-form are classified as noise in this experiment. This noise tends to obscure the response due to the propagation of the wave-form generated by application of the pulse load. In this study, two methods are used to minimize the effect of noise on the measured signal. First, the signals from individual tests are "stacked" (averaged). Since noise is, in general, seen in the measurements as a random process, averaging has the effect of increasing the ratio of the signal to noise. Second, wavelet analyses incorporating statistical significance testing is applied to the "stacked" signals to identify those components of the response that are most likely to be caused by the propagation of the wave-form through the soil.

The approach combines wavelet analysis with statistical significance testing to identify the components in an acceleration record that are associated with the propagating wave-form and to remove components associated with noise. The wavelet selected for analyzing the measured acceleration time series is the complex Morlet wavelet. The complex Morlet consists of a plane wave modulated by a Gaussian, Equation 1.

$$\psi_0(\eta) = \pi^{-1/4} e^{-i\omega_0 \eta} e^{-\frac{\eta^2}{2}} \tag{1}$$

where ω_0, the non-dimensional frequency, is taken as 6 to satisfy admissibility conditions for wavelets (Farge 1992). The continuous wavelet transform of a discrete sequence, x_n is defined as the convolution of x_n with a scaled and translated version of $\psi_0(\eta)$ (Torrence and Compo 1998), as shown in Equation 2.

$$W_n(s) = \sum_{n'=0}^{N-1} x_{n'} \psi^* \left[\frac{(n' - n)\delta t}{s} \right] \tag{2}$$

where the (*) indicates the complex conjugate. By varying the wavelet scale, s, and translating along the localized time index n, a picture is developed that shows both the amplitude of any features in the time series versus the scale and how this amplitude varies with time. The subscript 0 on ψ is dropped to indicate that ψ has been normalized.

Use of Equation 2 yields wavelet coefficients in both time and scale (frequency). The resulting wavelet coefficients are used to compute the signal's power in time-frequency space. The complex wavelet transform can be divided into the real part, $\Re\{W_n(s)\}$, the imaginary part, $\Im\{W_n(s)\}$, the amplitude $|W_n(s)|$, and phase, $\tan^{-1}\left[\Im\{W_n(s)\}/\Re\{W_n(s)\}\right]$. Finally, the wavelet power spectrum is defined as $|W_n(s)|^2$.

Torrence and Compo (1998) propose developing an expected value for $|W_n(s)|^2$ which is equal to N times the expected value for $|x_k|^2$, where x_k represents a discrete time series for the noise. For a white noise time series, this expectation value is $\frac{\sigma^2}{N}$, where σ^2 is the variance in the time series. The expected value of the wavelet transform is $|W_n(s)|^2 = \sigma^2$ at all n and s for this case. For this study, noise is included as measurements of accelerations generated by ambient or background noise.

Torrence and Compo (1998) show that the local wavelet spectrum follows the mean Fourier spectrum and that because the original Fourier components are normally distributed, the wavelet coefficients are also normally distributed and the wavelet power spectrum, $|W_n(s)|^2$, is χ_2^2 distributed. Assuming a mean background spectrum, at each time n and scale s, the distribution for the local wavelet power spectrum is, Equation 3.

$$\frac{|W_n(s)|^2}{\sigma^2} \Rightarrow \frac{1}{2} P_k \chi_2^2 \tag{3}$$

The value of P_k is the mean spectrum at the Fourier frequency that corresponds to the wavelet scale s. After finding an appropriate background spectrum and choosing a confidence level for χ_2^2, such as 95%, Equation 3 can be used at each scale to compute desired confidence levels.

The statistically significant coefficients are used to reconstruct the signal. This process removes those acceleration measurements associated with noise, leaving a signal that is highly likely to be associated with passage of the wave-form. Torrence and Compo (1998) present a simple reconstruction methodology using a delta function. Since the wavelet transform is a bandpass filter with a known response function (the wavelet function), it is possible to reconstruct the original time series using either deconvolution or the inverse filter. This is complicated by the redundancy in time and scale for the continuous wavelet transform. However, the redundancy makes it possible to reconstruct the time series using an entirely different wavelet function, the easiest of which is a delta (δ) function (Farge 1992). Using the delta function, the reconstructed time series is just the sum of the real part of the wavelet transform over all scales:

$$x_n = \frac{\delta j \delta t^{1/2}}{C_\delta \psi_0(0)} \sum_{j=0}^{J} \frac{\Re\{W_n(s_j)\}}{s_j^{1/2}} \tag{4}$$

where C_δ is a constant for each wavelet function.

The measured signal in the vertical direction at 1.22m from the source is compared to the reconstructed signal in Figure 4 for the case where a 15.2cm x 15.2cm x 76cm concrete beam is buried 15cm (depth to top of beam) in the soil. As shown, the main character and detail of the wave-form is maintained while variations in the signal at times away from the traverse of the pulse are strongly attenuated (t=0.15 to 0.25 sec.). The shape of the wave-form shown in Figure 4 is consistent with the shape of the Rayleigh wave computed analytically following Mooney (1974) for propagation of waves through soil media.

The reconstructed acceleration signals can be used to make comparisons between responses at sensor locations for cases having no inclusion and cases where inclusions are buried in the soil. From these comparisons, the effect of the inclusion on the form of the resulting wave can be inferred by associating differences in response to the dynamic response of the inclusion. This assumes elastic behavior and superposition of waves created by the impulse on the free-field (case without inclusion) and waves created by vibration of the inclusion. An example of changes in wave form is shown in Figure 5 for a location beyond the inclusion, at a distance of 1.22m from the source, to demonstrate the effect of the change in signal that is caused by the wave traveling and interacting with the embedded body. The upper plot shows the two acceleration time histories overlain on the same time scale while the lower plot shows the difference between the two measurements. The upper plot

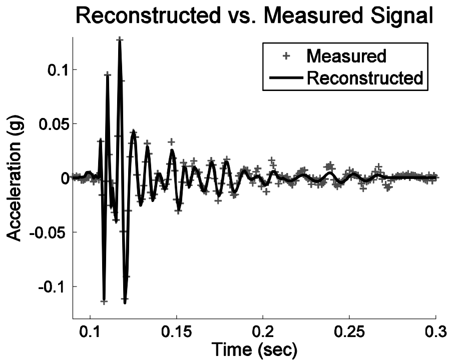

Figure 4: Comparison of measured and reconstructed wave-form

demonstrates the phase shift caused by interaction of the wave with a denser, stiffer material. The lower plot reveals direct evidence that the wave is changed by the presence of an inclusion. While this is not surprising, the degree of difference in signals is easily seen. Measurements at other locations give similar results where the differences between "free-field" and "inclusion" is easily and consistently measurable.

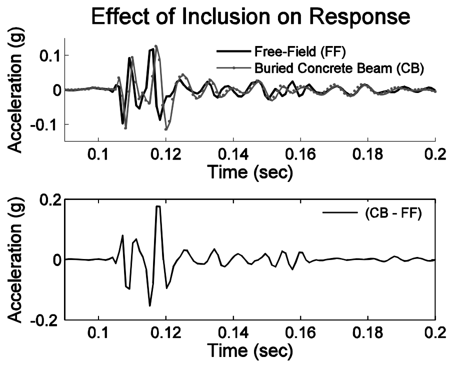

Figure 5: Effect of inclusion on wave-form at 1.22 m from source

In addition to filtering noise from measured signals, Shokouhi, et al. (2005) used the results of axi-symmetric finite element analyses to demonstrate that wavelet time-frequency (CWT) maps of the signal can be developed that identify arrival times and frequency ranges of incident and reflected wave-forms. An example of Shokouhi's (2005) results is shown in Figure 6, where the arrival of compression, shear and surface waves are identified as I, II, and III, respectively. Energy due to reflected waves occurs later in the time signal and is identified as regions IV and V. A similar approach has been used to develop wavelet time-frequency maps for measured acceleration data obtained from the experiments. A typical result is shown in Figure 7 where results of wavelet analysis are presented as contour plots with x and y axes representing time and frequency. Wavelet CWT maps of measured horizontal (radial) responses from an accelerometer positioned at L=1.22m for free-field and beam-inclusion cases are shown. Although in the measured data, separation of wave types cannot be easily discerned, the changes in wavelet amplitude caused by the beam-inclusion are unmistakable and reflect the time delay and frequency shift observed in Figure 5. Peak magnitudes for free-field are located approximately at 0.109 sec and 240 Hz while the beam-inclusion has a peak at 0.117 sec and 110 Hz. Note that the distributions have very different shapes. This is due to the beam's interference of waves in these frequency ranges. The shift and spreading to higher time values is analogous to phaseshifts of surface waves measured by SASW methods.

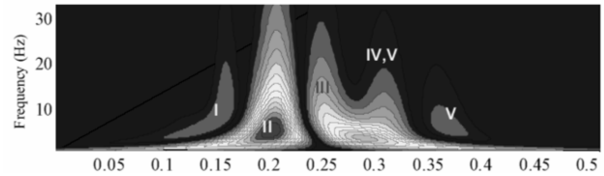

Figure 6: Wavelet CWT map for cavity, (after Gucunski (2005))

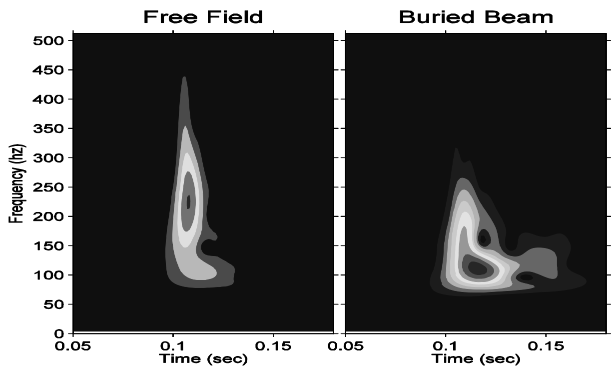

Figure 7: Wavelet CWT map for free-field and buried beam measured data

5 CONCLUSIONS

The model experiment demonstrates that the use of MEMS technology for data collection permits recording high quality spatial and temporal data needed to characterize changes to wave propagation caused by inclusion of bodies in a uniform media. Wavelets are a useful tool for highlighting important characteristics of measured wave propagation and characterizing changes to the propagation for differing conditions. Presently, research is focused on mapping wave characteristics throughout the entire testing region to aid in determining location, shape and material properties of inclusions.

ACKNOWLEDGEMENT

Wavelet software was provided by C. Torrence and G. Compo, and is available at URL: http://paos.colorado.edu/research/wavelets.

REFERENCES

Farge, M. 1992. Wavelet transforms and their applications to turbulence. *Annual Review of Fluid Mechanics* 24 (January): 395-458.

Gucunski, N, and P. Shokouhi. 2005. Wavelet transforms in surface wave analysis. In *Proceedings of the Sessions of the Geo-Frontiers 2005 Congress Austin, Texas, USA.* Soil Dynamics Symposium in Honor of Professor Richard D. Woods (GSP 134). Austin, TX, USA: ASCE.

Mooney, Harold M. 1974. Some numerical solutions for Lamb's problem. *Bulletin of the Seismological Society of American* 64, no. No. 2, April: 473-91.

Shokouhi, P, N. Gucunski, and A. Maher. 2005. Dynamic signatures of cavities and buried objects obtained from surface wave testing. In *Proceedings of the Sessions of the Geo-Frontiers 2005 Congress Austin, Texas, USA.* Geo-Frontiers 2005, vol. Earthquake Engineering and Soil Dynamics (GSP 133). Austin, TX, USA: ASCE.

Torrence, Christopher, and Gilbert P Compo. 1998. A practical guide to wavelet analysis. *Bulletin of the American Meteorological Society* 79: 61